THE ASTRONOMICAL JOURNAL, 119:126–135, 2000 January
© 2000. The American Astronomical Society. All rights reserved. Printed in U.S.A.

YOUNG STELLAR NUCLEI IN THE LENTICULAR GALAXIES. II. NGC 7280[1]

V. L. AFANASIEV
Special Astrophysical Observatory, Nizhnij Arkhyz, 357147 Russia; vafan@sao.ru
AND
O. K. SIL'CHENKO[2]
Sternberg Astronomical Institute, Moscow, 119899 Russia; and Isaac Newton Institute, Chile, Moscow Branch; olga@sai.msu.su
Received 1999 June 3; accepted 1999 October 1

ABSTRACT

We have undertaken bidimensional spectroscopy of the central part of the nearby lenticular galaxy NGC 7280 with the Multi-Pupil Fiber Spectrograph of the 6 m telescope of the Special Astrophysical Observatory. We find a rather young stellar nucleus, with a mean population age of 1.5 ± 0.5 Gyr, which is more metal-rich than the bulge at $R \approx 1$ kpc by an order of magnitude. The chemically and age-decoupled nucleus seems to be spatially resolved: the circumnuclear absorption index isolines represent ellipses elongated in P.A. $\approx 100°$–$110°$. The same orientation, P.A. $= 103°$, is found for the elongated circumnuclear stellar structure, revealed from the morphological analysis of the *Hubble Space Telescope* (*HST*) WFPC2 and NICMOS images of NGC 7280 and seen best of all at $R = 1''$. Taking into account the stellar kinematics inside $R \approx 2''$, we conclude that this structure is a circumnuclear stellar disk inclined with respect to the global plane of the galaxy. Meanwhile, both photometric and kinematical data in the radius range $2''$–$8''$ imply the existence of an intermediate-scale bar elongated in P.A. $\approx 60°$. The circumnuclear ionized gas is distributed and rotates in the plane orthogonal to the plane of the circumnuclear stellar disk.

Key words: galaxies: nuclei — galaxies: individual (NGC 7280) — galaxies: evolution — galaxies: structure

1. INTRODUCTION

Integrated photometric and spectral properties of early-type galaxies imply that their major stellar population is very old, almost as old as the universe. But the center of a galaxy is a special place; the stellar nucleus may have a particular evolution that differs from the evolution of the whole galaxy. By analyzing statistics of photoelectric multiaperture photometry of nearby galaxies (Sil'chenko 1994), we have found that in at least 25%–30% of all elliptical and lenticular galaxies, the nuclei are distinguished from the surrounding spheroids by a prominently red color. We have interpreted this phenomenon as being due to a significant fraction of chemically distinct stellar nuclei in early-type galaxies.

Chemically distinct galactic nuclei are still poorly studied; their relation to a global galactic structure is quite unclear, and so any speculations on their origin are somewhat premature. However, there were some hints about the relation between the chemically distinct nuclei in elliptical galaxies and the presence of fast-rotating circumnuclear stellar disks (Bender & Surma 1992; Surma & Bender 1995; Scorza & Bender 1995; Forbes, Franx, & Illingworth 1995). On the other hand, a correlation between the absorption-line index Hβ and the fourth Fourier coefficient a_4 has been noted in elliptical galaxies, so that elliptical galaxies with inner disks have younger (on average) stellar populations (de Jong & Davies 1997). The resulting picture is consistent with the occurrence of secondary star formation bursts in the centers of some elliptical galaxies that produced compact circumnuclear stellar disks whose mean age is younger and mean metallicity is higher than those of the main galactic spheroids. The full set of these properties—higher nuclear metallicity, younger nuclear age, and photometric signatures of circumnuclear disks—are directly observed in the elliptical galaxies NGC 4365 (Bender & Surma 1992; Surma & Bender 1995; Carollo et al. 1997a) and NGC 4621 (Sil'chenko 1997). Similar coincidence of the chemically, morphologically, and dynamically decoupled entities has also been found in the center of the lenticular galaxy NGC 4816 (Mehlert et al. 1998).

We think that lenticular galaxies are more promising for studying the connection between chemical distinctness, young age, and diskiness of decoupled galactic cores. First, their stellar nuclei are on average younger than the nuclei of elliptical galaxies; among nearby lenticulars, 50% show prominent Balmer absorption lines Hγ and/or Hδ in their nuclear spectra, implying a mean stellar age of less than 5 billion years (Sil'chenko 1993a). Second, the same fraction, 50%, of nearby lenticulars appear to have separate circumnuclear stellar disks embedded in extended bulges (Seifert & Scorza 1996). In the first paper of this series (Sil'chenko 1999a, hereafter Paper I) we studied two lenticular galaxies with chemically decoupled nuclei, NGC 1023 and NGC 7332. We have detected intermediate-age stellar populations in the centers of these galaxies. The mean stellar age in the nucleus of NGC 1023 is 7 billion years, and in the nucleus of NGC 7332 it is 2.5 ± 0.5 billion years. Moreover, the intermediate-age stellar structures in the centers of these lenticulars are not pointlike. An enhanced Hβ absorption line is observed up to $2''$ from the center in NGC 1023 and up to $5''$ from the center in NGC 7332. The sizes of the intermediate-age stellar structures coincide with the sizes of embedded circumnuclear stellar disks, so for these galaxies the connection between chemically and evolutionarily decoupled cores and separate circumnuclear disks seems to

[1] Partly based on observations collected with the 6 m telescope at the Special Astrophysical Observatory (SAO) of the Russian Academy of Sciences (RAS).
[2] Guest Investigator of the RGO Astronomy Data Centre

TABLE 1

GLOBAL PARAMETERS OF NGC 7280

NGC Parameter (Source)	Value
Type (NED)	SAB(r)0+
R_{25} (LEDA)	8.6 kpc
B_T^0 (LEDA)	12.64
M_B (LEDA)	−19.45
$B-V$ (RC3)	0.85
$U-B$ (RC3)	0.37
V_r(radio) (LEDA)	1846 ± 14 km s^{-1}
Distance (LEDA, $H_0 = 75$ km s^{-1} Mpc^{-1})	26.3 Mpc
Inclination (LEDA)	52°
P.A.$_{phot}$ (LEDA)	78°
σ_0 (LEDA)	111 km s^{-1}
v_m (LEDA)	130 km s^{-1}

be quite probable. The target of the second stage of this work, the lenticular galaxy NGC 7280, is rather gas-rich; about 10^9 $M_\odot$ neutral hydrogen has been detected in it (Biermann, Clarke, & Fricke 1979; Chamaraux, Balkowski, & Fontanelli 1987). It possesses an irregular companion galaxy 3.′7 (∼28 kpc) from it, which makes some interaction with a gas accretion possible in the past. However, now no traces of star-forming activity (namely, no Hα emission) are observed in either the disk or the nucleus of NGC 7280 (Pogge & Eskridge 1987, 1993).

The global parameters of the galaxy are given in Table 1. We report our observations and other data used in § 2. The photometric structure of the central part of NGC 7280 is studied in § 3, and the kinematical analysis is presented in § 4. The radial variations of the stellar population properties are analyzed in § 5, and § 6 gives our conclusions.

2. OBSERVATIONS AND DATA REDUCTION

In 1998 we undertook two-dimensional spectroscopy of NGC 7280 with the Multi-Pupil Fiber Spectrograph (MPFS) of the 6 m telescope of the Special Astrophysical Observatory (Nizhnij Arkhyz, Russia). The blue-green spectral range, 4250–5600 Å, was exposed on August 17, and the red spectral range, 5650–7000 Å, was exposed on October 16. The exposure times were 60 minutes for each spectral range (3 × 20). A grating of 1200 grooves mm^{-1} was used, which provided a reciprocal dispersion of 1.3 Å per pixel and a spectral resolution of 3 Å. On both dates a seeing of FWHM = 2″ was estimated.

These spectral observations have been made with the new variant of the panoramic spectrophotometer, which began to work at the prime focus of the 6 m telescope at the end of 1997. With respect to the previous variants of MPFS (Afanasiev et al. 1990, 1996), the field of view is now increased, and the common spectral range is larger as a result of using fibers, which transmit light from 16 × 16 square elements of the galaxy image to the slit of the spectrograph (256 fibers) together with the sky background taken in 4.′5 off the galaxy itself (6 fibers). The size of one spatial element is 1″ × 1″. At the exit of the spectrograph a 1024 × 1024 CCD registers all the 262 spectra simultaneously. The primary reduction of the data is made within IDL. After bias-subtracting, flat-fielding, and extracting one-dimensional spectra from the CCD frame, we linearize and analyze each spectrum individually. The one-element spectral characteristics, such as fluxes in continuum or in emission lines, redshift, and absorption-line indices are then combined into two-dimensional arrays corresponding to the galactic region under consideration, with the help of software developed earlier at the Special Astrophysical Observatory (SAO; Vlasyuk 1993) and with our own FORTRAN programs. To calculate absorption-line indices and their errors, we have also used the FORTRAN program of A. Vazdekis. As a result, we obtain two-dimensional surface brightness distributions, velocity fields, and maps of stellar population characteristics. In the blue-green spectral range, we measure the absorption-line indices Hβ, Mg b, Fe λ5270, and Fe λ5335 in the popular Lick system (Worthey et al. 1994); to check the consistency of our measurements with the model indices calculated in this system (Worthey 1994), we also observed stars from their list (Worthey et al. 1994). In addition, we use our blue-green spectra to derive a stellar velocity field in the center of NGC 7280 by cross-correlating elementary galactic spectra with the spectrum of a K-giant star, the brighter component of the visual binary ADS 15470. In the red spectral range, we have measured barycenter positions of the emission line [N II] λ6583 to derive a velocity field of the ionized gas (Hα emission is absent in NGC 7280). We have estimated the best accuracy of our velocity measurements as 6 km s^{-1} from the night-sky line [O I] λ6300 analysis. As for the absorption-line index accuracy, we have made estimates using the method of Cardiel et al. (1998); the typical error of the indices varies from 0.15 Å in the nucleus to 0.6 Å for the individual elements at the edges of the area investigated. To keep a constant level of accuracy along the radius, we summed the spectra in concentric rings centered on the nucleus and studied the radial dependencies of the absorption-line indices by comparing them to synthetic models of the old stellar populations of Worthey (1994) and Tantalo, Chiosi, & Bressan (1998). We estimate the mean accuracy of our azimuthally averaged indices as 0.1 Å. To give an impression on our data quality, the azimuthally averaged spectra are displayed in Figure 1.

The photometric data involved in our analysis are taken from the La Palma and *Hubble Space Telescope* (*HST*) archives.

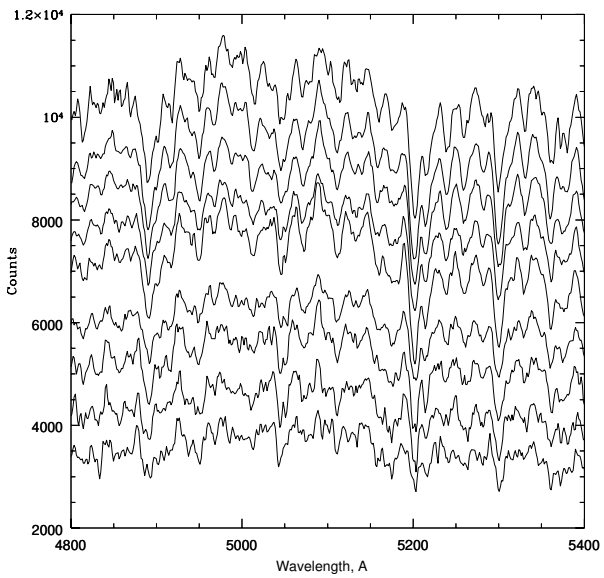

FIG. 1.—Azimuthally averaged spectra obtained with the MPFS for NGC 7280. The corresponding radii are 0″, 1.″0, 2.″0, 3.″0, 4.″0, 5.″0, 6.″0, 7.″0, and 8.″0 (*top to bottom*). The normalizations and shifts are arbitrary.

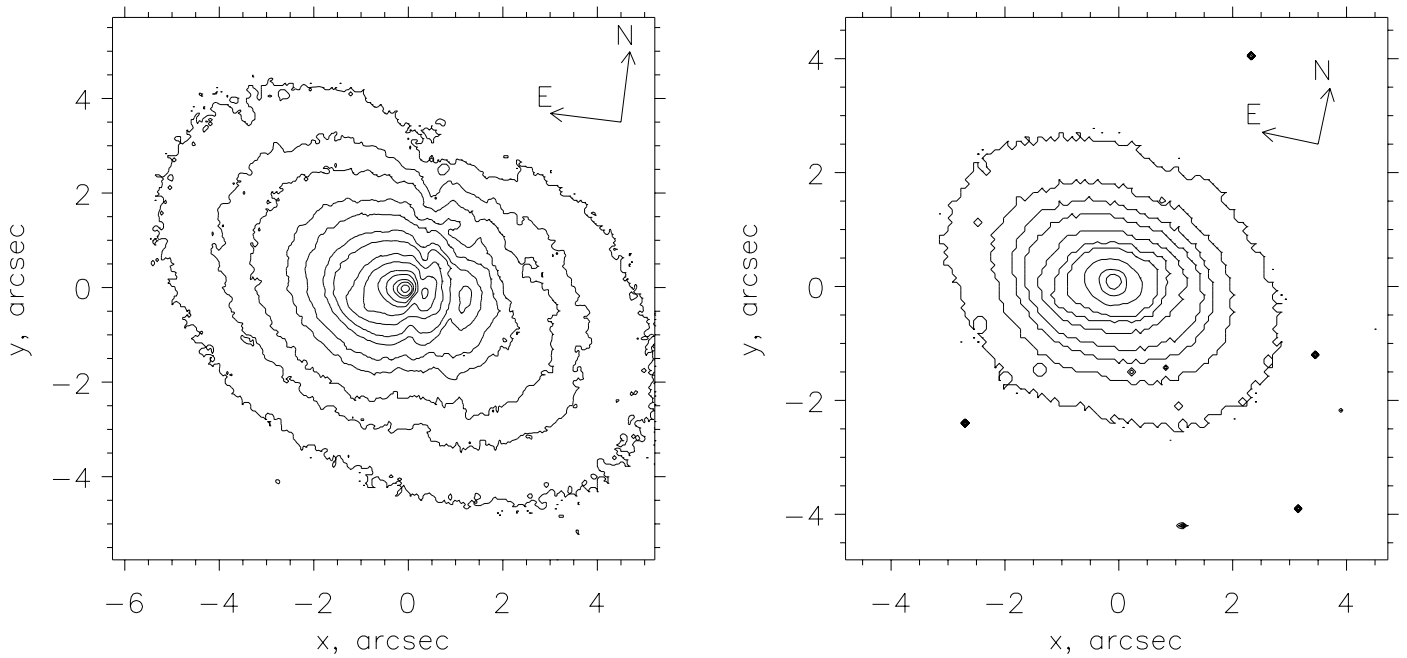

FIG. 2.—Isophotes in the central part of NGC 7280 obtained with the *HST* WFPC2 through F606W (*left*) and the *HST* NICMOS2 through F160W (*right*).

The broadband *R* image of NGC 7280 was obtained on 1992 May 28 at the 1 m Jacobus Capteyn Telescope on La Palma. The minimum exposure time was 10 minutes, and the very center, inside $R \approx 1''.5$, is saturated. The seeing quality is estimated from the neighboring star measurements as FWHM = 1".5. The central part of the galaxy has been observed by the *HST* (PI, M. Stiavelli; program 6359). It has been exposed with the WFPC2 through the wide optical-band filter F606W for 600 s (400 + 200) on 1996 December 1, and with the NICMOS2 through the filter F160W for 128 s on 1997 December 27. The spatial resolution was 0".1 and 0".2, respectively. We have derived morphological characteristics of the surface brightness distribution in NGC 7280 by analyzing these images; the program FITELL of V. V. Vlasyuk has been used for this purpose.

3. STRUCTURE OF THE CENTRAL PART OF NGC 7280

Figure 2 presents a direct view of the central part of NGC 7280 in the optical (*left*) and near-infrared bands (*right*) obtained with high spatial resolution at the *HST*. In the left panel of Figure 2, the most prominent features are two narrow dust lanes almost perpendicular to the major axis of the continuum distribution; they are located 0".3 and 1".0 to the west of the center and elongated in the north-south direction. Carollo et al. (1997b) described the configuration of this dust complex as "dust lane wraps several times around nucleus." In the near-infrared (Fig. 2, *right*) the dust is invisible, making the turn of isophotes in the very center quite evident. This turn can also be suspected from the left panel of Figure 2; light excess in the west–east direction gives an appearance of an inclined compact circumnuclear disk superposed on the smooth spheroidal brightness distribution.

This impression has been confirmed by morphological analysis of the isophotes. Figure 3 presents radial variations of the major-axis position angle and ellipticity if the isophotes are approximated by ellipses. Orientation of the global line of nodes of the galaxy is 78° according to RC3 and 74° according to Lu (1998); we have obtained $P.A._0 = 72°$ at our outermost point, $R \approx 45''$. However, in the central part of the galaxy the orientation of the isophotes is quite different: at $R = 1''$, P.A.(*r*) has a maximum, 103°, that is well measured both from the WFPC2 and from the NICMOS data, and at $R \approx 9''$, P.A.(*r*) has a minimum at 58°. The latter feature is accompanied by a local maximum of ellipticity, ~0.4. In general, we note that the isophotes of

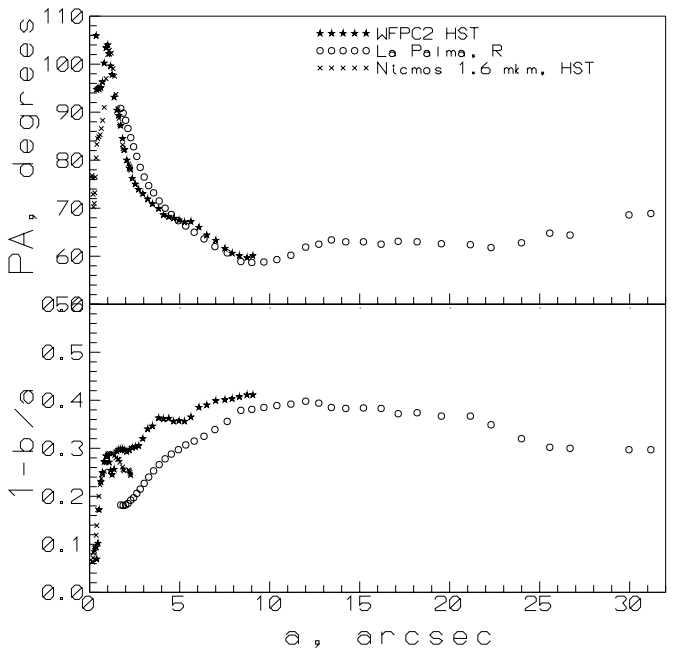

FIG. 3.—Radial variations of the isophote morphological characteristics in the center of NGC 7280 according to the *HST* data (*stars*) and the La Palma data (*open circles*).

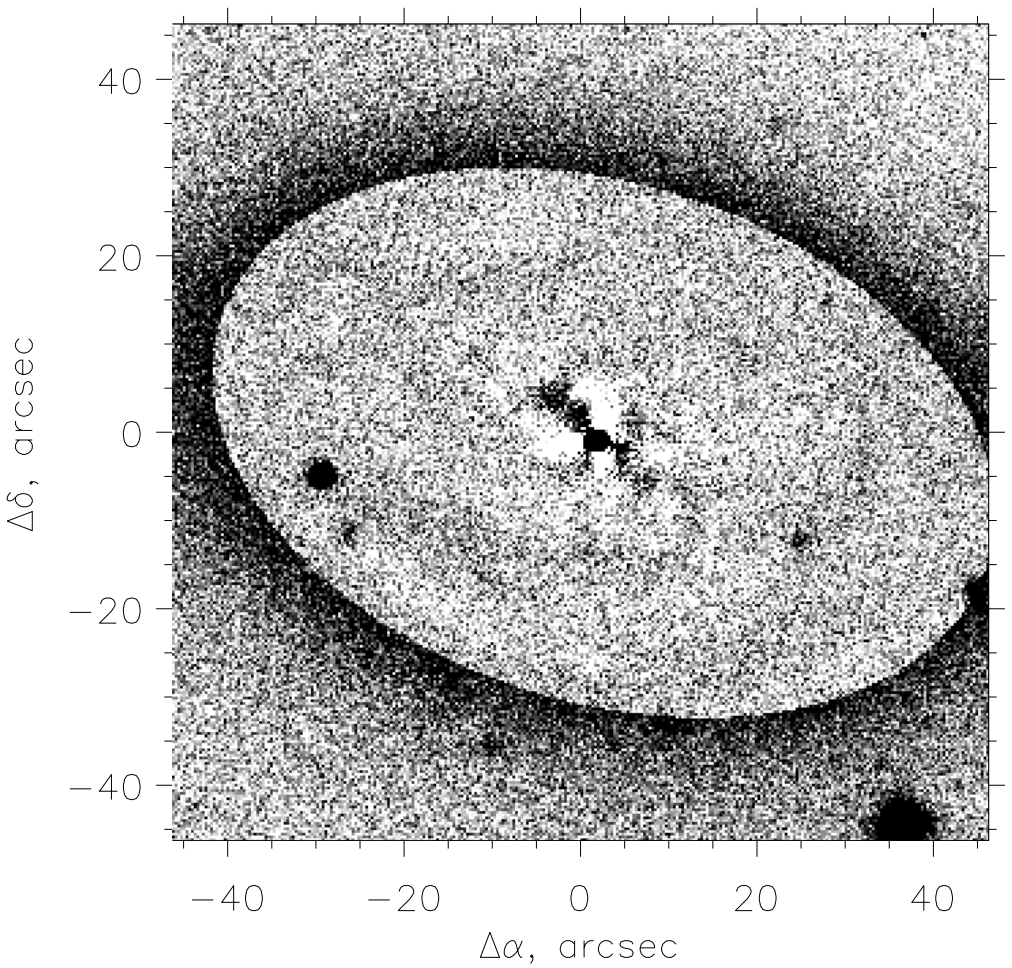

FIG. 4.—Residual brightness map of the central part of NGC 7280, obtained from the La Palma JKT *R* image by subtracting the pure ellipsoidal brightness distribution. North is up, east is to the left; the black spot in the center marks the nucleus position, and the light ellipse borders the area where the model has been subtracted.

NGC 7280 are rather highly elongated even close to the center: $1 - b/a = 0.3$ is already achieved at $R = 1''$, and the maximum ellipticity appropriate for a thin disk under the inclination of NGC 7280, $i = 52°$ (see Table 1), would be 0.38 (indeed, 0.356 is measured by Lu 1998). Such behavior of the ellipticity is rather strange in a lenticular galaxy with a prominent bulge. Figure 4 shows a map of residual *R*-band brightness after the subtraction of pure elliptical isophotes with the parameters plotted in Figure 3. The circumnuclear substructure elongated in P.A. = 103° cannot be seen here because of the saturation of the central 2″ on the La Palma image, but one can clearly see the substructure with a radius of ∼9″ elongated in P.A. ≈ 60°. The substructure looks asymmetric; the northeastern part is brighter than the southwestern one. This seems natural if we extrapolate circumnuclear dust skewness toward the west (Fig. 2, *left*) onto the larger scale. In general, the substructure resembles a strong, although low-contrast, bar, which is seen almost edge-on, and to the southwest of the nucleus, where the receding edge of the bar is the nearest to us (see § 4), we see it through the dust lane.

All of the above concern the stellar surface distribution. However, using the MPFS data we have also constructed a map of the surface brightness distribution for the emission line [N II] λ6583 (Fig. 5), hoping that it reflects a distribu-

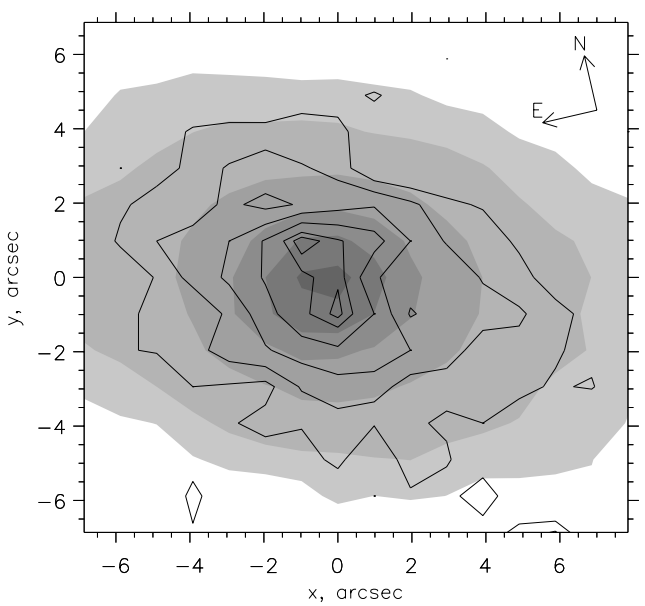

FIG. 5.—Surface brightness distribution for the emission line [N II] λ6583 (*isolines*) superimposed on the gray-scaled red continuum map, which is in logarithmic units. The nitrogen brightness units are not calibrated; within the peaks the counts are about 60, and the isoline step is 5.

tion of the ionized gas. Although this map involves only the central part of the galaxy, 16″ × 16″, the distribution of the ionized gas emission looks complex; there is an overall elongation in P.A. ≈ 60°, but inside this distribution there is also compact circumnuclear substructure with a diameter of ∼3″ elongated perpendicularly to the major axis of continuum isophotes (the separation of two emission brightness peaks is statistically insignificant). Remembering that circumnuclear dust lanes are also aligned perpendicularly to the continuum isophote major axis, we can suppose the existence of the orthogonal circumnuclear diffuse matter disk or bar. To make a choice between them, we need kinematical data, which is discussed in the next section.

4. KINEMATICS OF THE IONIZED GAS AND STARS IN THE CENTER OF NGC 7280

Figure 6 presents isovelocities for stars (*left*) and ionized gas (*right*) superimposed on the continuum image of the central part of NGC 7280. Even at first glance, both velocity fields look rather complex; isovelocities are twisted beyond the close vicinity of the nucleus, and this kinematical peculiarity confirms our hypothesis about the medium-scale bar implied by the photometric data reviewed in the previous section. However, in the very center, the regular behavior of the stellar isovelocities allows us to suppose an axisymmetric solid-body rotation. The gaseous isovelocities near the center of NGC 7280 are almost aligned along the major axis of the continuum isophotes, that is, perpendicular to the stellar isovelocities. This fact, together with the nitrogen emission brightness distribution (Fig. 5) and crossing dust lanes (Fig. 2, *left*), strengthens our idea that the gaseous dusty circumnuclear disk settles and rotates in the plane orthogonal to the global plane of the galaxy.

Let us try to more precisely determine the parameters of the stellar and gaseous rotation around the nucleus of NGC 7280. Under the assumption of plane axisymmetric rotation, the azimuthal dependence of central line-of-sight velocity gradients must be a cosine one,

$$dv_r/dr = \omega \sin i \cos (\text{P.A.} - \text{P.A.}_0) ,$$

where ω is the deprojected central angular rotation velocity, i is the inclination of the rotation plane, and P.A._0 is the orientation of the line of nodes coinciding in the case of an axisymmetrical ellipsoid (or a thin disk) with the photometric major axis.

In axisymmetrically rotating stellar or gaseous systems with moderate inclination, $i = 40°$–$60°$, fitting of the observed azimuthal dependence of the circumnuclear line-of-sight velocity gradients by a cosine law is a powerful tool for determining rotation plane orientation and for estimating angular rotation velocity. Figure 7 presents such dependencies for the stars and ionized gas in the center of NGC 7280, measured at two different distances from the nucleus. First, one can make sure once more that outside $R > 2''$ the evident noncircular motions disturb regular rotation, particularly gas rotation; the azimuthal dependence for $R = 2''.0$–$3''.1$ demonstrates characteristic "waves" around the best-fit cosinusoid, revealing the presence of higher-order harmonics in the velocity field. However, inside $R \approx 2''$ (almost unresolved scale in our observations) the cosinusoids are rather good. The corresponding best-fit formulae are

$$dv_r/dr = [20 \cos (\text{P.A.} - 262°) + 2.0] \text{ km s}^{-1} \text{ arcsec}^{-1}$$

for the stars, and

$$dv_r/dr = [64 \cos (\text{P.A.} - 9°) + 1.9] \text{ km s}^{-1} \text{ arcsec}^{-1}$$

for the gas, under the assumption that our measured systemic velocity is 1860 km s^{-1}. One can see that the rotation plane of the ionized gas is indeed roughly orthogonal to the rotation plane of the stars. We have already argued that the gas rotation looks circular because the emission-line brightness distribution and the dust lanes are aligned in the same position angle as the "dynamical major axis" of the gas. But the same argument must be also applied to the stellar

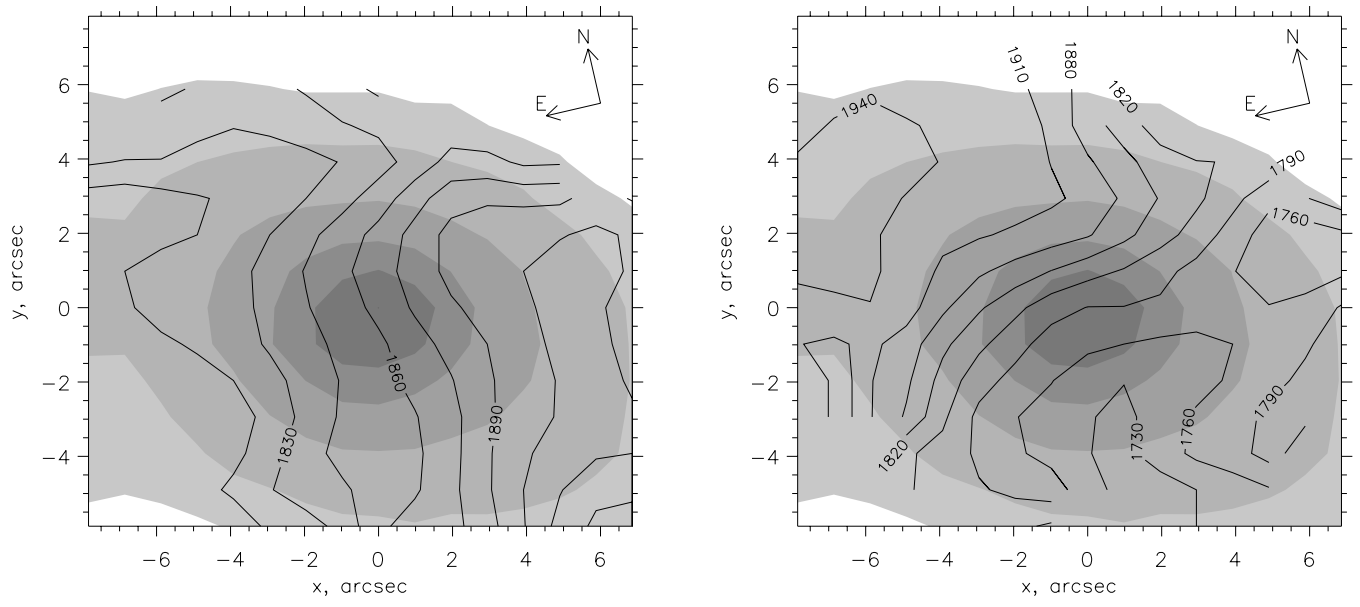

FIG. 6.—Isovelocities in the centers of NGC 7280 for the stellar component (*left*) and the ionized gas (*right*). The isovelocities are superimposed on the gray-scaled continuum distributions.

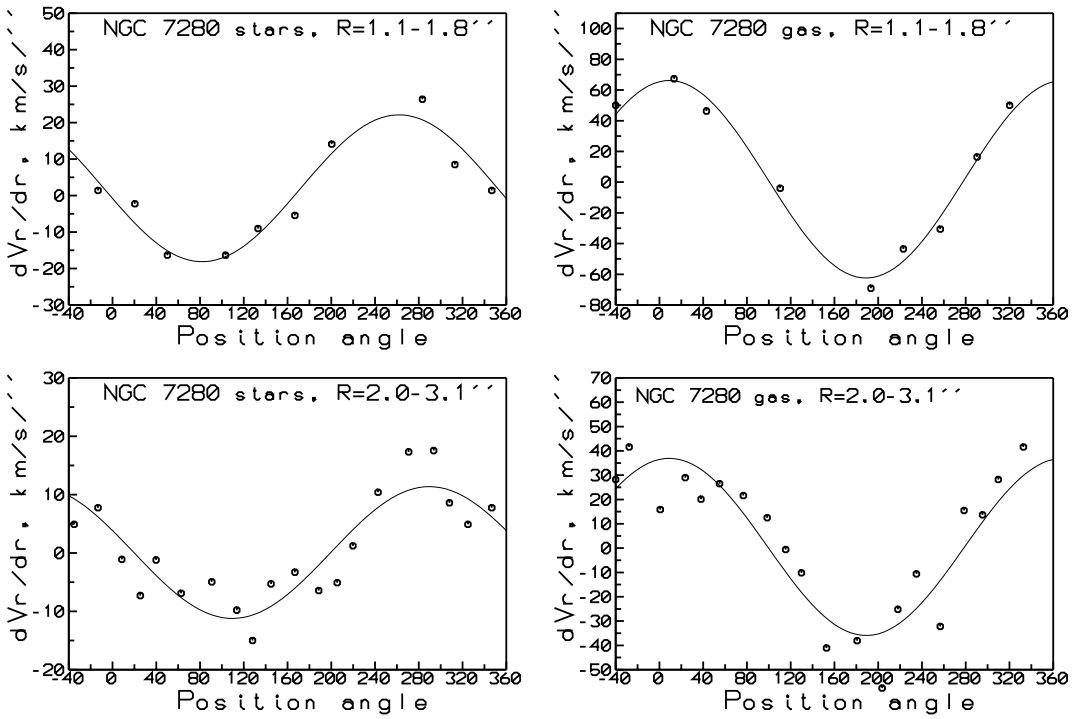

FIG. 7.—Azimuthal dependencies of the central line-of-sight velocity gradients for the stars (*left*) and ionized gas (*right*) in NGC 7280 in two radial bins; solid lines show the best-fit cosinusoids.

rotation. Its dynamical major axis, P.A. = 82°, coincides exactly with the photometric major axis at the corresponding distance from the center (Fig. 3), and this is a signature of axisymmetric rotation: in the presence of a triaxial potential, the dynamical and photometric major axes must turn in opposite directions with respect to the line of nodes (Monnet, Bacon, & Emsellem 1992). In the meantime, in the center of NGC 7280 the dynamical and photometric major axes are turned in the same direction, by $\sim +10°$ with respect to the line of nodes; this means that we deal with a compact ($R \leq 200$ pc) circumnuclear stellar disk inclined with respect to the global galactic plane. If we refer to the high-resolution photometric data of *HST* (Fig. 3), the tilt of the circumnuclear stellar disk may reach at least 30°.

It is interesting to compare the angular rotation velocities of the stars and ionized gas. The amplitude of the cosinusoid for the stars is lower than the amplitude for the ionized gas by a factor of 3 (Fig. 7). If we assume that we see the circumnuclear gaseous disk edge-on, while the circumnuclear stellar disk is seen more open, e.g., under $i = 52°$, just as the global disk, then the difference in the angular rotation velocities would be reduced only slightly, by a factor of 2.5. The stellar velocity dispersion in the center of NGC 7280 is too low (see Table 1) to support a slowly rotating bulge. We can propose only one possible explanation for the visible slow rotation of the stellar component: in the presence of a global bar, a noticeable counterrotating stellar component may exist (for theoretical evidence, see Wozniak & Pfenniger 1997; for observational evidences for NGC 2841, see Afanasiev & Sil'chenko 1999; for NGC 7331, see Prada et al. 1996 and Sil'chenko 1999b). Under our moderate spectral resolution, we cannot separate kinematical substructures with velocities close enough ($\Delta v_r \leq 200$ km s^{-1}); instead, we measure line-of-sight velocities artificially lowered by the presence of an unresolved counterrotating stellar component.

Considering the above conditions, we would like to use the rotation velocity of the ionized gas as a more reliable estimator of the mass contained inside the radius of solid-body rotation. If we take this radius to be equal to 2″ (which is in reality an upper limit), we obtain $v_{\rm rot} = 128$ km s^{-1} at $R = 2''$ and a corresponding mass within this radius of $\sim 10^9\ M_\odot$. This value of the rotation velocity achieved at only 0.26 kpc from the center is almost exactly equal to the half-width of the H I 21 cm line (Chamaraux et al. 1987). This means that the mass is strongly concentrated in the center. Statistically, the central angular rotation velocity of the ionized gas of 500 km s^{-1} kpc^{-1} and the central mass concentration of $\sim 10^9\ M_\odot$ are quite typical for disk galaxies with dynamically decoupled nuclei (Afanasiev, Sil'chenko, & Zasov 1989); the nontypical feature is the confinement of rotation to the circumnuclear polar ring.

5. PROPERTIES OF THE STELLAR POPULATION IN THE CENTER OF NGC 7280

Figure 8 shows two-dimensional distributions of the absorption-line indices Mg *b* (*top*), $\langle$Fe$\rangle \equiv$ (Fe λ5270 + Fe λ5335)/2 (*middle*), and Hβ (*bottom*). The metal-line indices, as well as Hβ, are strongly peaked in the nucleus of the galaxy. However, the region of enhanced absorption lines seems to be spatially resolved; the central isolines of all three indices represent ellipses elongated in P.A. $\approx 100°$–$110°$. The Hβ distribution has one additional peak to the southwest of the center; being elongated in P.A. = 60°/240°, it may have originated from a site of recent star formation at the receding edge of the global bar. The Mg *b* map demonstrates a rather lumpy central structure; the compact spots are statistically significant, but we have no idea as to

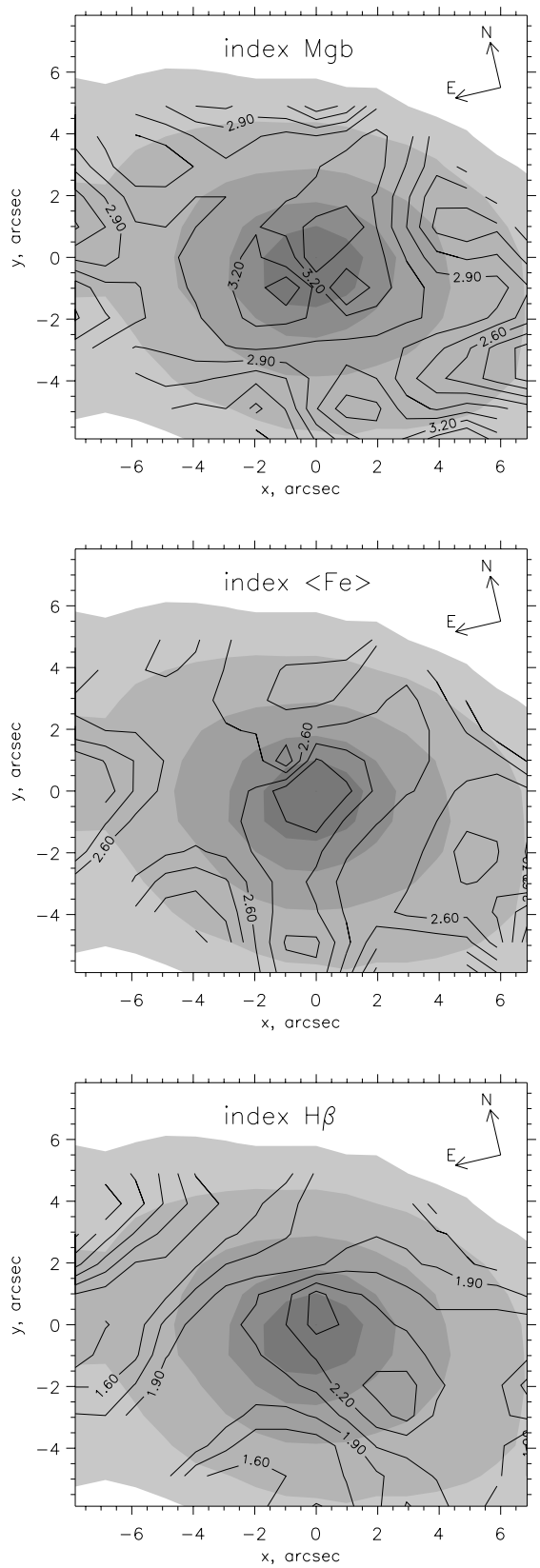

FIG. 8.—Two-dimensional distributions in the central part of NGC 7280 for the Lick index Mg *b*, in Å (*top*), the Lick index ⟨Fe⟩, in Å (*middle*), and the Lick index Hβ, in Å (*bottom*). The isolines representing the absorption-line indices are superimposed on the gray-scaled green continuum map. The statistical errors of the indices are about 0.1–0.15 Å in the center and about 0.6 Å at the edges; the outer parts of the maps at $R > 3''$ were smoothed by a Gaussian with FWHM = 2.″5 (seeing quality) for a better presentation.

their possible origin. However, the circumnuclear ellipses in distributions of all three indices are quite similar: evidently, we see a metal-enriched and rather young elongated circumnuclear stellar structure. Its orientation, P.A. $\approx 100°$–$110°$, coincides exactly with the orientation of the photometric circumnuclear stellar disk (see Fig. 3), but the photometric disk is more compact than the chemically and age-decoupled structure; the radius of the former is 1″, while the latter feature extends up to $R \approx 3''$. One can argue that the spatial resolutions of the *HST* data presented in Figure 3 and the MPFS data presented in Figure 8 are too different. However, the continuum isophotes plotted in Figure 8 are obtained under the same resolution as the index maps, and at $R = 2''$–$3''$ they look elongated in P.A. $\approx 80°$, an orientation quite different from that of the index isolines. We can propose the following explanation for this difference: while the surface brightness of the circumnuclear disk (and its contribution to the total surface brightness) drops rapidly with the radius, the stellar population properties in the disk must become more extreme, that is, the age must fall and the metallicity must increase, to keep a more shallow radial change of the integrated stellar properties. This means that the secondary star formation burst finished earlier in the nucleus and later in the circumnuclear disk. Other examples of such sequences of the secondary star formation bursts in galactic centers are the S0 galaxy NGC 1023 (Sil'chenko 1999a) and the Sb galaxy NGC 7331 (Sil'chenko 1999b).

To determine physical characteristics of the stellar population in the center of NGC 7280, we must compare the observed absorption-line indices to model results. In doing this there are two difficulties. First, the accuracy of index measurements drops rapidly with the distance from the center. If the random error of 0.15 Å in the nuclear indices allows us to determine stellar population parameters with a sufficient reliability, corresponding roughly to a metallicity accuracy of 0.1 dex and an age accuracy of 1 Gyr (if its absolute value is near 2–3 Gyr), increasing the typical error even to 0.3 Å makes any efforts in this direction quite ineffective. Therefore, we cannot construct useful two-dimensional maps of the stellar population parameters. Instead, we prefer to average index measurements in concentric rings with the center in the nucleus and a width of 1″, and to analyze radial dependencies of the age and metallicity. The accuracy of the azimuthally averaged indices is better than 0.1 Å, except at the outermost point, where it is 0.2 Å. The second difficulty is that most stellar population models are calculated for solar element ratios, while in real galaxies these ratios may be nonsolar. For example, elliptical galaxies are known to be magnesium-overabundant with respect to the iron abundance (Worthey, Faber, & Gonzalez 1992). There have also been claims that the bright lenticulars are similar to ellipticals of the same luminosity and have [Mg/Fe] > 0 (Fisher, Franx, & Illingworth 1996); however, our preliminary analysis shows evidence for a rather solar magnesium-to-iron ratio in all disk galaxies, including lenticulars (Sil'chenko 1993b). In any case, we prefer to check the magnesium-to-iron ratio of any individual galaxy. In Paper I, we have ascertained that the bulges in NGC 1023 and NGC 7332 demonstrate solar Mg/Fe, while the nuclei are both chemically decoupled and appear to be different: the younger nucleus in NGC 7332 has [Mg/Fe] = 0, and the older nucleus in NGC 1023 is magnesium-overabundant, [Mg/Fe] $\approx +0.3$. The situation

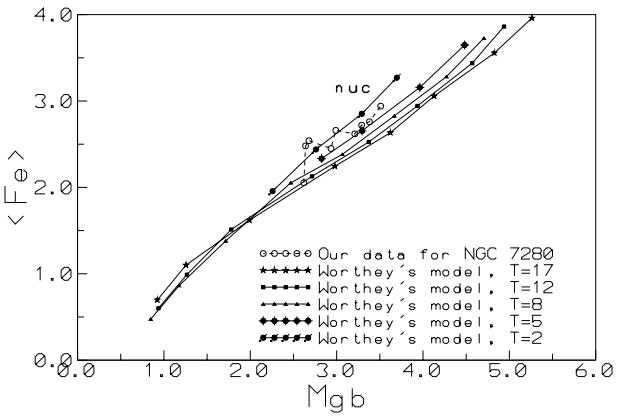

FIG. 9.—Diagram (⟨Fe⟩ vs. Mg *b*) for NGC 7280. The measurements are azimuthally averaged and taken along the radius with the step of 1.″0. The ages of the Worthey (1994) models are given in Gyr.

in NGC 7280 can be clarified with the help of Figure 9; on the ⟨Fe⟩ versus Mg *b* diagram, we compare the indices observed in NGC 7280 in the radius range 0″–8″ with the stellar population models of Worthey (1994), calculated under the assumption of a solar magnesium-to-iron ratio. One can see that in the center of NGC 7280, despite of the overall metallicity gradient, the solar Mg/Fe ratio is conserved everywhere. This conclusion remains valid for the nucleus of NGC 7280 even if it is younger than 5 Gyr. Therefore, the results of an analysis of Figure 9 assure us that we can safely use models with a solar magnesium-to-iron ratio, particularly the popular models of Worthey (1994), to determine the age of the stellar population at the center of NGC 7280.

Figure 10 presents a set of age-diagnostics diagrams, in which we compare our azimuthally averaged measurements with the models of old stellar populations: the Hβ versus Mg *b* diagram with the models of Worthey (1994) (*top*), Hβ versus [MgFe] $\equiv$ (Mg *b* ⟨Fe⟩)$^{1/2}$ with the models of Worthey (1994) (*middle*), and Hβ versus ⟨Fe⟩ with the models of Tantalo et al. (1998) for [Mg/Fe] = 0 (*bottom*). All three comparisons give consistent results. The nucleus of NGC 7280 is very young; the mean age of the stellar population is 1.5 Gyr. The mean stellar age increases radially outward; between $R = 2''$ and $R = 5''$ it oscillates (remaining roughly constant?) between 5 and 8 Gyr, and at $R > 5''$ it suddenly rises to 12–17 Gyr. The behavior of the mean metallicity anticorrelates with that of the mean age. The stellar population in the nucleus is super–metal-rich, $[m/\mathrm{H}] \geq +0.5$. Moving along the radius, the metallicity decreases; in the intermediate-age "belt" at $R = 2''$–$5''$ it is roughly solar, and in the old "bulge" at $R = 6''$–$8''$ it falls below -0.5. The full range of the metallicity variations between the center and $R = 8''$ ($\sim$1 kpc) is an order of magnitude. This is an unprecedented fall compared to the smooth metallicity gradients seen in early-type galaxies (Davies, Sadler, & Peletier 1993; Carollo, Danziger, & Buson 1993), but we have found the same metallicity drop by an order of magnitude in the lenticular galaxy NGC 7332 (Sil'chenko 1999a), where this phenomenon is related to the presence of the decoupled circumnuclear stellar disk.

6. CONCLUSIONS AND DISCUSSION

In the lenticular galaxy NGC 7280 we have found a rather young stellar nucleus, with a mean stellar population

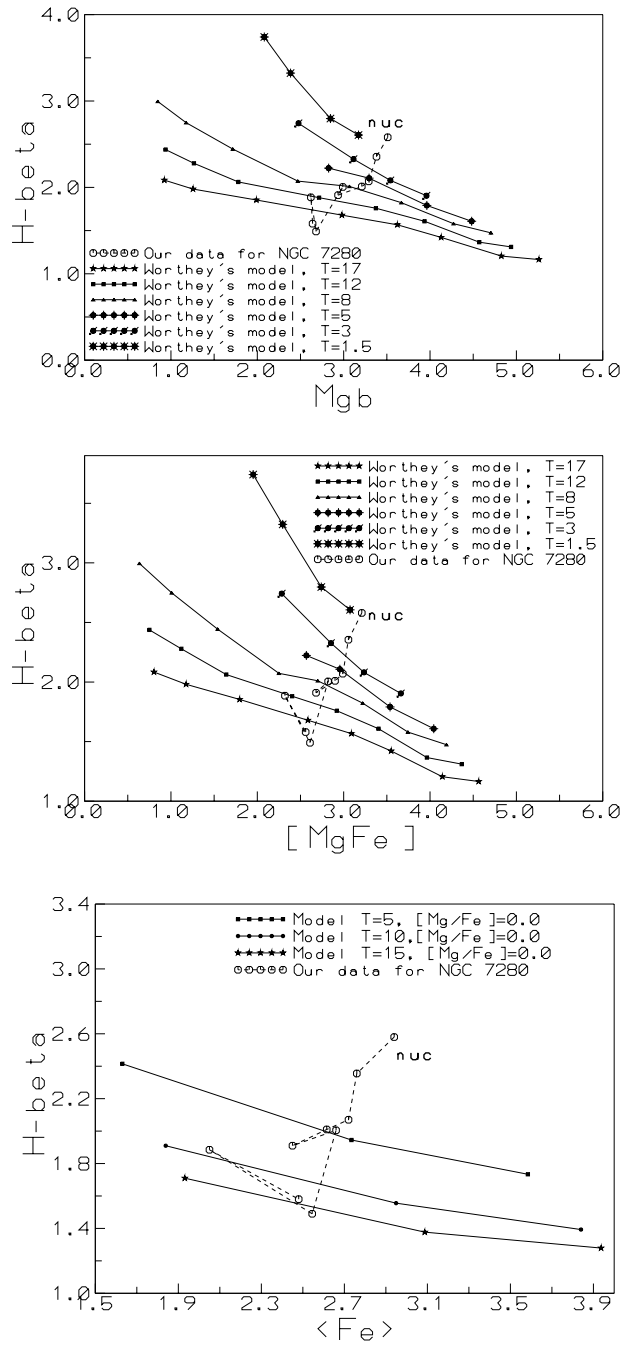

FIG. 10.—Age diagnostics diagrams for NGC 7280. *Top*: Hβ vs. Mg *b*, the models of Worthey (1994). *Middle*: Hβ vs. [MgFe], the models of Worthey (1994). *Bottom*: Hβ vs. ⟨Fe⟩ for [Mg/Fe] = 0, the models of Tantalo et al. (1998). The measurements are azimuthally averaged and taken along the radius with the step of 1.″0. The ages of the models are given in Gyr; the metallicities for Worthey's models are +0.50, +0.25, 0.00, −0.22, −0.50, −1.00, −1.50, and −2.00, if one takes the signs from right to left, and for the models of Tantalo et al. they are +0.4, 0.0, and −0.7.

age of 1.5 $\pm$ 0.5 Gyr, which is more metal-rich by an order of magnitude than the bulge at $R \approx 1$ kpc. The statistical error of the nuclear age estimate is obtained by projecting error bars of the metal and Balmer line indices onto the line of equal metallicity, $[m/\mathrm{H}] = +0.5$. In general, there may be a systematic age error related to a Balmer emission confusion of the absorption-line index Hβ. Some early-type galaxies demonstrate a narrow emission line Hβ at the

bottom of the broader absorption line, and this effect may result in age overestimation through the artificial diminution of the absorption-line index Hβ. However, we have already mentioned that in NGC 7280 the measurable Balmer emissions are absent. We have tried to estimate an upper limit on the possible systematic error due to Hβ emission. The equivalent width of the noiselike emission feature at the position of redshifted Hα (which is always the strongest among the Balmer emission lines) is less than 0.3 Å at $R \leq 5''$ and less than 0.6 Å at $R = 6''$–$7''$. Since the continuum is almost flat between 4800 and 6600 Å, this means that the equivalent width of the Hβ emission, if it exists, is less than 0.1 Å at $R \leq 5''$ and less than 0.2 Å at $R = 6''$–$7''$, and this is a possible correction for the emission that should be applied to the absorption-line index Hβ. For the nucleus of NGC 7280, it means that the possible age systematic error due to Hβ emission is less than 0.1 Gyr.

The age of the stellar populations that we determine here is not, of course, an absolute age value; our estimate must be considered in the frame of the stellar isochrone sets that are used in model calculations. Particularly, Worthey (1994) used the stellar isochrones of VandenBerg and coworkers and revised Yale isochrones that were calculated in the mid-1980s. Since then some improvements have been made in this field; particularly, the necessity of taking into account mild overshooting has been proved. This effect is important for stars more massive than 1.6 $M_\odot$ or for stellar systems younger than 4–5 Gyr (Maeder & Meynet 1991), and therefore is important for the nucleus of NGC 7280. The possible systematic error of the age estimate due to neglecting the overshooting effect can be evaluated by the analogy with open star clusters of similar ages. Carraro et al. (1993) have measured the ages of two intermediate-age ($1 < T < 2$ Gyr) open clusters, NGC 752 and NGC 3680, by comparing observed *C-M* diagrams with the theoretical isochrones calculated with and without overshooting; they have found that including overshooting increases the age estimates by 0.4 Gyr. Therefore, the age estimate for the nucleus of NGC 7280 must perhaps be increased up to 2 Gyr if one refers to the state-of-art stellar evolution theory.

The chemically and age-decoupled nucleus seems to be spatially resolved; the circumnuclear absorption index isolines represent ellipses elongated in P.A. $\approx 100°$–$110°$. The same orientation, P.A. = 103°, is found for the elongated circumnuclear stellar structure seen best at $R = 1''$, the existence of which has been revealed by morphological analysis of the *HST* WFPC2 and NICMOS images of NGC 7280. Taking into account the stellar kinematics inside $R \approx 2''$, we conclude that this structure is a circumnuclear stellar disk inclined with respect to the global plane of the galaxy. In the meantime, both photometric and kinematical data in the radius range $2''$–$8''$ imply the existence of an intermediate-scale bar elongated in P.A. $\approx 60°$. Interestingly, the circumnuclear ionized gas is distributed and rotates in the plane orthogonal to the plane of the circumnuclear stellar disk.

The main problem that has attracted our attention for some years is the origin of decoupled nuclei. Is it possible to form a decoupled nucleus without capturing "external" matter, or does its presence always signify merging in the past? When we found a circumnuclear "polar" gaseous disk similar to what we report now in NGC 7280 in the regular Sb galaxy with the chemically decoupled nucleus NGC 2841 (Sil'chenko, Vlasyuk, & Burenkov 1997), we concluded that it was a result of past gas accretion. But later, having made an analysis of the global structure and kinematics of this galaxy, we ascertained that it has a triaxial bulge that can explain all the spectacular phenomena observed in NGC 2841, including the counterrotating stellar component and the circumnuclear gaseous polar ring (Afanasiev & Sil'chenko 1999). Moreover, the majority of circumnuclear stellar disks accompanying the presence of the decoupled nuclei lie in the main galactic planes (M31, Sil'chenko, Burenkov, & Vlasyuk 1998; NGC 4216 and 4501, Sil'chenko et al. 1999; NGC 1023, Sil'chenko 1999a), so there is no reason to think that they are products of accreted material consumption. However, the case of NGC 7280 strongly complicates the picture. We observe several populated planes in the center of this galaxy; neither the plane of the circumnuclear stellar disk nor the plane of the circumnuclear gaseous disk coincides with the main galactic plane. There is a global bar in NGC 7280, but we cannot identify any populated circumnuclear planes with the principal planes of this triaxial structure. Perhaps we have encountered for the first time a transient situation in the center of an early-type galaxy related to some cyclic interaction with the gas-rich satellite galaxy. Both bar and decoupled circumnuclear disk may be produced by this interaction, but by *different* episodes of this interaction. A tidally induced bar forms during several rotation periods (Miwa & Noguchi 1998), which are only 10^7 yr in the center of NGC 7280; in the mean while, the decoupled nuclear disk is approximately 10^9 years old. In such a case they are not obliged to be related geometrically. We would also like to stress that the decoupled nucleus in NGC 7280 is the youngest of all the ones found by us, so this galaxy may be quite unique in the evolution of its central region structure.

We thank the astronomers of the Special Astrophysical Observatory S. N. Dodonov and A. V. Moiseev for supporting the observations at the 6 m telescope. The 6 m telescope is operated under the financial support of Science Ministry of Russia (registration number 01-43). During the data analysis, we have used the Lyon-Meudon Extragalactic Database (LEDA), supplied by the LEDA team at the CRAL-Observatoire de Lyon (France) and the NASA/IPAC Extragalactic Database (NED), which is operated by the Jet Propulsion Laboratory, California Institute of Technology, under contract to NASA. This research has made use of the La Palma Archive. The telescope JKT is operated on the island of La Palma by the Royal Greenwich Observatory at the Spanish Observatorio del Roque de los Muchachos of the Instituto de Astrofisica de Canarias. The work is partly based on observations made with the NASA/ESA *Hubble Space Telescope*, obtained from the data archive at the Space Telescope Science Institute, which is operated by the Association of Universities for Research in Astronomy, Inc., under NASA contract NAS5-26555. We have also used the software ADHOC, developed at the Marseille Observatory, France. The work was supported by a grant of the Russian Foundation for Basic Researches 98-02-16196, by a grant of the President of Russian Federation for young Russian doctors of sciences 98-15-96029, and by the Russian State Scientific-Technical Program "Astronomy: Basic Space Researches" (Astronomy section).

REFERENCES

Afanasiev, V. L., Dodonov, S. N., Drabek, S. V., & Vlasyuk, V. V. 1996, MPFS Manual (Nizjnij Arkhyz: SAO)
Afanasiev, V. L., & Sil'chenko, O. K. 1999, AJ, 117, 1725
Afanasiev, V. L., Sil'chenko, O. K., & Zasov, A. V. 1989, A&A, 213, L9
Afanasiev, V. L., Vlasyuk, V. V., Dodonov, S. N., & Sil'chenko, O. K. 1990, preprint (SAO N54)
Bender, R., & Surma, P. 1992, A&A, 258, 250
Biermann, P., Clarke, J. N., & Fricke, K. J. 1979, A&A, 75, 7
Cardiel, N., Gorgas, J., Cenarro, J., & Gonzalez, J. J. 1998, A&AS, 127, 597
Carollo, C. M., Danziger, I. J., & Buson, L. 1993, MNRAS, 265, 553
Carollo, C. M., Franx, M., Illingworth, G. D., & Forbes, D. A. 1997a, ApJ, 481, 710
Carollo, C. M., Stiavelli, M., de Zeeuw, P. T., & Mack, J. 1997b, AJ, 114, 2366
Carraro, G., Bertelli, G., Bressan, A., & Chiosi, C. 1993, A&AS, 101, 381
Chamaraux, P., Balkowski, C., & Fontanelli, P. 1987, A&AS, 69, 263
Davies, R. L., Sadler, E. M., & Peletier, R. F. 1993, MNRAS, 262, 650
de Jong, R. S., & Davies, R. L. 1997, MNRAS, 285, L1
Fisher, D., Franx, M., & Illingworth, G. 1996, ApJ, 459, 110
Forbes, D. A., Franx, M., & Illingworth, G. D. 1995, AJ, 109, 1988
Lu, N. Y. 1998, ApJ, 506, 673
Maeder, A., & Meynet, G. 1991, A&AS, 89, 451
Mehlert, D., Saglia, R. P., Bender, R., & Wegner, G. 1998, A&A, 332, 33
Miwa, T., & Noguchi, M. 1998, ApJ, 499, 140
Monnet, G., Bacon, R., & Emsellem, E. 1992, A&A, 253, 366
Pogge, R. W., & Eskridge, P. B. 1987, AJ, 93, 291
———. 1993, AJ, 106, 1405
Prada, F., Gutierrez, C. M., Peletier, R. F., & McKeith, C. D. 1996, ApJ, 463, L9
Scorza, C., & Bender, R. 1995, A&A, 293, 20
Seifert, W., & Scorza, C. 1996, A&A, 310, 75
Sil'chenko, O. K. 1993a, AZh. Pis'ma, 19, 693
———. 1993b, AZh. Pis'ma, 19, 701
———. 1994, AZh, 71, 706
———. 1997, AZh, 74, 643
———. 1999a, AJ, 117, 2725 (Paper I)
———. 1999b, AJ, 118, 186
Sil'chenko, O. K., Burenkov, A. N., & Vlasyuk, V. V. 1998, A&A, 337, 349
———. 1999, AJ, 117, 826
Sil'chenko, O. K., Vlasyuk, V. V., & Burenkov, A. N. 1997, A&A, 326, 941
Surma, P., & Bender, R. 1995, A&A, 298, 405
Tantalo, R., Chiosi, C., & Bressan, A. 1998, A&A, 333, 419
Vlasyuk, V. V. 1993, Izv. SAO RAS, 36, 107
Worthey, G. 1994, ApJS, 95, 107
Worthey, G., Faber, S. M., & Gonzalez, J. J. 1992, ApJ, 398, 69
Worthey, G., Faber, S. M., Gonzalez, J. J., & Burstein, D. 1994, ApJS, 94, 687
Wozniak, H., & Pfenniger, D. 1997, A&A, 317, 14